Lasers in Eng., Vol. 18, pp. 95–105
Reprints available directly from the publisher
Photocopying permitted by license only

Studies on Laser Surface Melting of Al-11% Si Alloy

A. BISWAS[1], B. L. MORDIKE[2], I. MANNA[1] AND J. DUTTA MAJUMDAR[1,*]

[1]*Dept. of Met. & Mat. Engg., Indian Institute of Technology, Kharagpur, WB-721302, India*
[2]*IWW, Agricola Strasse 6, D-38678 Clausthal-Zellerfeld, Germany*

In the present investigation the effect of laser surface melting on wear and corrosion resistance of Al-11 wt.% Si alloy has been investigated. Laser surface melting has been carried out using a 2 kW continuous wave CO_2 laser at an applied power of 2.3 kW and scan speed ranging from 6 to 12 mm/min. Following the laser surface melting, a detailed investigation of the melted zone in terms of microstructure, composition and phases were undertaken. Mechanical properties of the melted zone were evaluated so far as the microhardness and wear resistance were concerned. The corrosion behaviour of the as-received and the laser surface melted surface was evaluated in 1(M) H_2SO_4, 1(M) HNO_3 and 3.56 wt.% NaCl solutions. The microstructure of the melt zone consists of grain refined Al and Al-Si eutectic colonies which results in an improved microhardness from 87 VHN as compared to 55 VHN of the as-received Al-Si alloy. The wear resistance of the melt surface was improved significantly as compared to the as-received Al-Si alloy. A detailed corrosion study in various environments showed that corrosion resistance was marginally less in the 3.56 wt.% NaCl and 1 M H_2SO_4 solutions, but was better in the 1 M HNO_3 solution.

Keywords: Aluminium, silicon, laser, melting, wear, corrosion.

INTRODUCTION

Aluminium alloys with silicon as a major alloying element have a wide range of applications in the automotive and aerospace industries and provide most of all shaped castings manufactured [1]. The mechanical properties can be improved by small additions of sodium or strontium [2]. However, the amount of the modifier is critical since over-modification results in reduced mechanical

*Corresponding author: E-mail: jyotsna@metal.iitkgp.ernet.in

properties. Furthermore, losses from the melt and the formation of undesirable intermetallic compounds, cause additional problems. Microstructural refinement may also be achieved by laser surface melting by the modification of the microstructure and/or composition in near-surface region of the component by melting using a high power laser beam as a source of heat [3, 4]. Among the notable advantages, laser assisted surface modification enables delivery of a controlled quantum of energy (1-30 J/cm^2) or power (10^4-10^7 W/cm^2) with a precise temporal and spatial distribution either in short pulses (10^{-3} to 10^{-12} s) or as a continuous wave (CW) [3–6]. The large temperature gradient across the boundary between the melted surface and underlying substrate results in rapid self-quenching and re-solidification with quench rates as high as 10^5 K/s and accompanied by re-solidification velocities up to 30 m/s [7]. In addition, the short processing time, flexibility in operation, economy in time/ energy/material consumption, shallow heat affected zone and precision are important advantages of laser assisted surface modification over conventional processes. Laser surface melting has been successfully employed to improve wear and corrosion resistance properties of commercial metals and alloys [6–8]. Noordhuis and Hosson [9] showed that laser surface melting improved the surface microhardness of Al-12% Si alloy from 60 to 125 VHN. Furthermore, shot peening followed by laser surface melting increased the surface microhardness further and changed the residual stress from tensile which is developed by laser surface melting to compressive. Wang *et al*. [10] undertook a detailed study of the effect of laser surface melting using a CO_2 laser to determine the microstructure and microhardness of a series of Al-Si alloys. The morphology of Si particles was changed from lath-like into coralline-like with significant refinement of the microstructures and an extension of the solid solubility of Si in Al and an improved microhardness. In an another study, Wong and Liang [11] showed that laser surface melting improved the corrosion resistance of Al-Si alloys in 10% H_2SO_4 and 10% HNO_3 solution. Allen *et al*. [12] studied the solidification behaviour of laser surface melted Al-26 wt.% Si alloys. It was observed that columnar or epitaxial regrowth develops under the condition of low interfacial undercooling. The nucleation kinetics analysis indicates that the nucleation of primary silicon restricts the domain of the coupled eutectic zone for silicon compositions greater than 20 wt.%. Watkins *et al*. [13] presented a detailed review of laser surface melting of Al and its alloys in enhancing surface properties. Laser surface remelting of the hypereutectic Al-20 and 30 mass% Si cast alloys with a continuous wave CO_2 laser was found to improve the wear resistance of these alloys. The microstructure of the laser-remelted layer consisted in fine primary Si particles, the primary α-Al matrix phase and a fine α-Al-Si eutectic phase. The hardness of the laser remelted layer increased gradually with a decrease in the primary Si particle size, which reached 140 HV at about 5 μm in the Al-30 mass% Si layer [14]

In the present study, an attempt has been made to improve the wear resistance of Al-Si alloys by melting the surface with a high power laser beam.

The detailed investigation includes characterization of microstructure, composition and phases of the melted zone and an evaluation of mechanical and electrochemical properties.

EXPERIMENTAL

Laser surface melting was carried out using a 10 kW continuous wave (CW) CO_2 laser with a beam diameter of 2 mm and Ar as shrouding gas (at a flow rate of 6 l/min) to avoid oxidation. The specimens were mounted on a water chilled copper block placed on a CNC controlled stage. The applied power was maintained at 2.3 kW in the present study. The scan speed was varied from 6 to 12 mm/min. After laser surface melting the microstructure (both the surface and cross section) of the melted zone was characterised by optical (OM) and scanning electron microscopy (SEM). The phases formed on laser surface melting were analysed by X-ray diffractometer (XRD). The microhardness of the top surface and the cross-section of the laser surface melted layer were measured using a Vickers microhardness tester with a 25 g applied load. The wear behaviour of surface alloyed mild steel was compared to that of the as-received one by a Friction and Wear monitor unit (model no: TR-208-M1) based on a pin on disc wear testing method with the specimen as disc and diamond pyramid indenter (120°) as pin. During wear testing, the pin was slides over the disk at 15 rpm and an applied load of 1 kg. During the test the cumulative depth of wear was measured as a function of time using Winducom 2003 software. The corrosion resistance of the specimens before and after laser surface melting was studied in 1 (M) H_2SO_4, 1(M) HNO_3 and 3.5% NaCl solution. The corrosion behaviour of the laser surface melted specimen was also compared to that of the non treated specimen by calculating the corrosion rate derived from the potentiodynamic polarisation study (in a 3.56 wt.% NaCl solution in air) [15]. A standard calomel electrode was used as a reference electrode and platinum mesh was used as the counter electrode. Polarisation was carried out from –700 to –100 mV(SCE) at a scan rate of 0.5 mV/s to construct the Tafel plots (logarithmic variation of current as a function of voltage) and to derive the anodic and cathodic Tafel constants [15]. The corrosion current (i_{corr}) was determined from the intersection of these two linear plots [15].

RESULTS AND DISCUSSIONS

A detailed analysis of the microstructure, composition and phases were undertaken for laser surface melted and as-received Al-Si alloys. In addition, the mechanical properties such as microhardness, wear resistance and corrosion resistance were evaluated. In this section, we shall discuss the characteristics and properties of the melted layer in detail.

FIGURE 1
Scanning Electron Micrograph of the as-received Al-Si alloy used in the present study.

Characterisation of the Melted Zone

Figure 1 shows the scanning electron micrograph of the top surface of the 'As-received Al-11wt.% Si alloy' used in the present study. The microstructure consists of primary coarse grained aluminium and the presence of eutectic Al-Si. The silicon morphology was typically lath like and an example of divorced eutectic [16].

Figures 2(a–c) show the scanning electron micrographs of the cross section of the laser surface melted Al-11 wt.% Si alloy treated at a power of 2.3 kW and a scan speed of (a) 6 mm/s, (b) 9 mm/s and (c) 12 mm/s. Figure 2 shows that laser surface melting causes the formation of a very thin melted zone with a uniform thickness. The thickness could be varied from 100 to 900 μm depending on the various combinations of applied power and scan speed. It could also be observed that the melted zone is continuous, homogeneous and defect free. There was no defect between the melted zone and the substrate. A detailed surface roughness measurement was made and its variation with the laser parameters showed that the surface roughness was varied from 5 to 10 μm under the present set of laser parameters. A significant refinement of the microstructure was also observed after laser surface melting. The microstructure consists of uniformly dispersed, highly refined silicon in an aluminium matrix. The degree of refinement was found to vary with the laser parameters. A close comparison between Figures 2(a) to 2(c) shows that the melted thickness decreases with an increase in scan speed. The decreased depth of melting at a higher scan speed is attributed to less energy being absorbed when the interaction time is short and simultaneously at a higher scan speed. Figure 3 shows the variation of the depth of melting of laser surface melted Al-11% Si alloy with a scan speed (with an applied power of 2.3 kW). In Figure 3 it can be seen that the thickness of melting varies from 300 to 800 mm and decreases with an increase in scan speed.

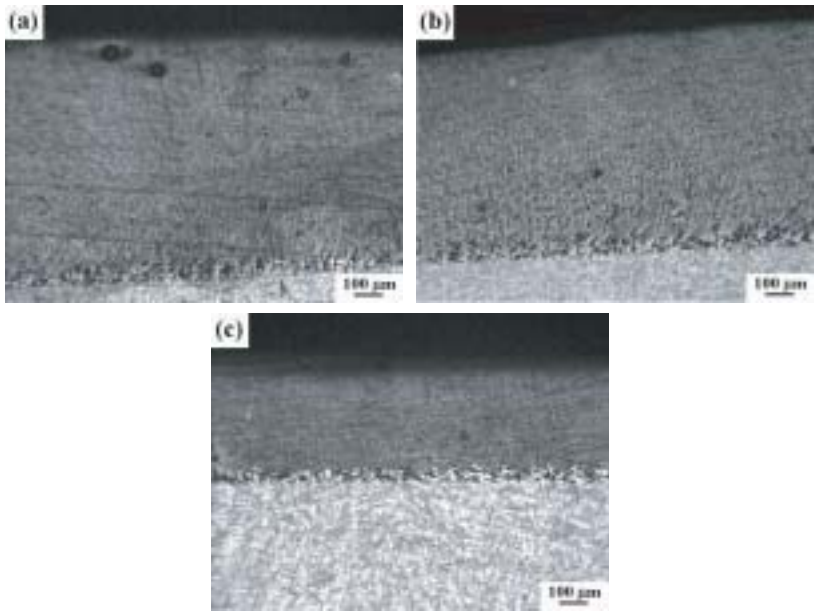

FIGURE 2
Scanning electron micrographs of the cross section of laser surface melted Al-11 wt.% Si alloy with an applied power of 2.3 kW and scan speed of (a) 6 mm/s, (b) 9 mm/s and (c) 12 mm/s.

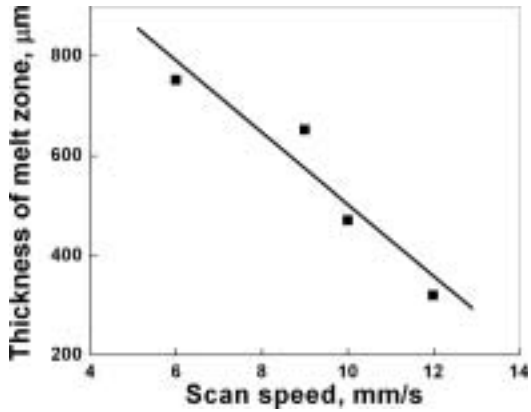

FIGURE 3
Variation of depth of melting with scan speed for laser surface melted Al-11 wt.% Si alloy (lased with a power 2.3 kW).

A detailed analysis of the microstructure of the cross section of the laser surface melted Al-Si alloy was carried out to study the effect of laser parameters on the interface of the melt zone. Figures 4(a–c) show the scanning electron micrographs of the interface between the melt zone and the substrate of laser

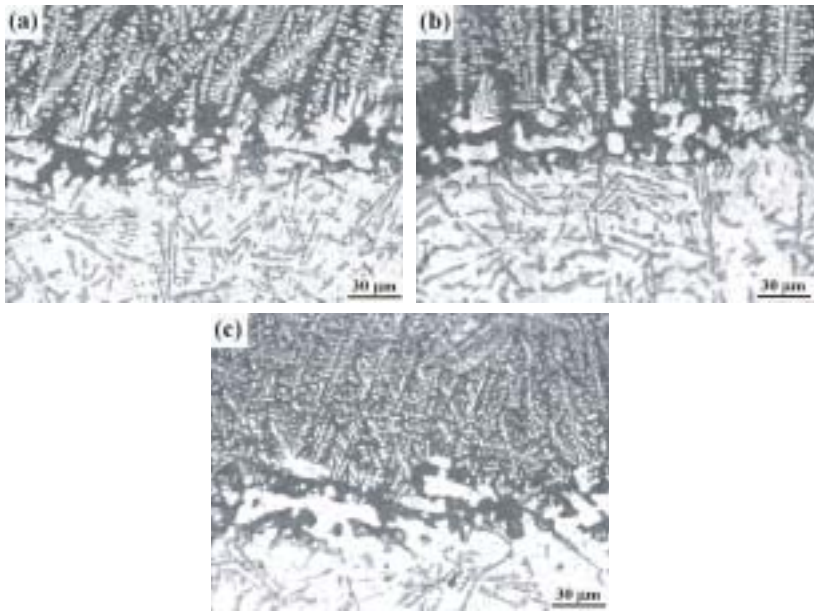

FIGURE 4
Scanning electron microstructures of the interface between the melt zone and substrate of laser surface melted Al-11 wt.% Si alloy lased at an applied power of 2.3 kW and scan speed of (a) 6 mm/s, (b) 9 mm/s and (c) 12 mm/s.

surface melted Al-11 wt.% Si alloy at an applied power of 2.3 kW and scan speed of (a) 6 mm/s, (b) 9 mm/s and (c) 12 mm/s. Figure 4 shows that the microstructures are predominantly dendritic at the interface. However, there is no solidification defect at the interface, despite rapid quenching. The direction of growth was mainly in the direction of the heat flow. A detailed comparison of secondary arm spacing shows that there is a marginal decrease in secondary arm spacing with increase in scan speed, which is attributed to a higher cooling rate at a lower interaction time. However, the growth direction did not change much while changing the scan speed.

Figures 5(a–c) show the scanning electron microstructures of the top surface of laser surface melted Al-11 wt.% Si alloy at a power of 2.3 kW and scan speed of (a) 6 mm/s, (b) 9 mm/s and (c) 12 mm/s. In Figure 5 the microstructures consist of very fine dendrites of Al and the presence of Al-Si eutectics in the interdendritic region. The secondary arm spacing of the dendrites were found to decrease marginally with an increase in scan speed. On the other hand, at a very high scan speed (12 mm/min), the microstructure changes from dendritic to cellular. There was a very high degree of refinement when applying the high scan speed. The morphology of eutectic silicon also changes from needle/lath like to very fine globular. Figure 6 shows the higher magnification view of the melt zone of the laser surface melted Al-11% Si alloy at a power of 2.3 kW

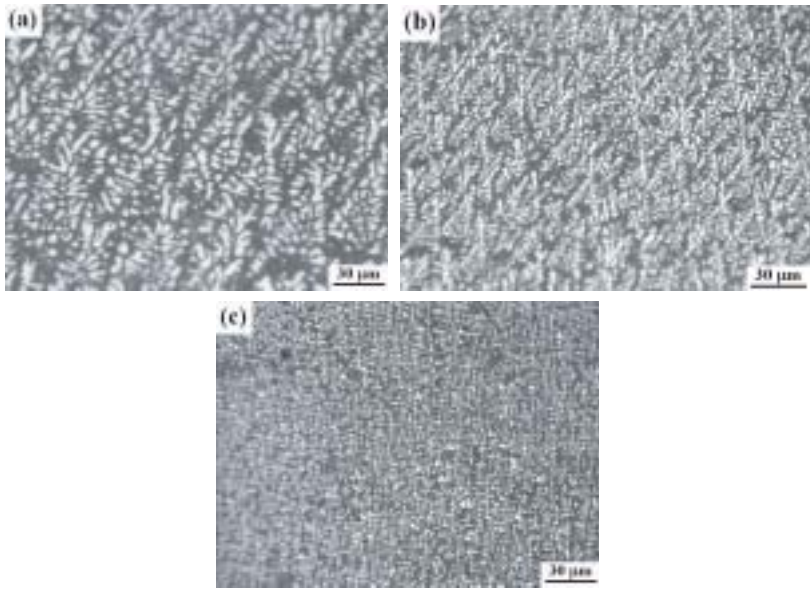

FIGURE 5
Scanning electron microstructures of the interface between the melt zone and substrate of laser surface melted Al-11 wt.% Si alloy lased at an applied power of 2.3 kW and scan speed of (a) 6 mm/s, (b) 9 mm/s and (c) 12 mm/s.

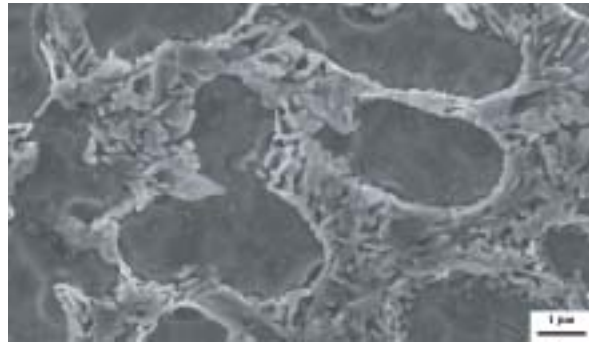

FIGURE 6
Scanning electron micrograph of the top surface of laser surface melted Al-11 wt.% Si alloy lased at an applied power of 2.3 kW and scan speed of 6 mm/s.

and scan speed of 6 mm/s. Figure 6 shows that eutectic phases are mostly present in the interdendritic region and morphologies of eutectic silicon are both globular and rosette like in nature. In this regard, it is relevant to note that the change in morphology of eutectic silicon from the lath-like form into a coralline-like form was reported by Wang et al. [10] during laser surface melting of Al-Si.

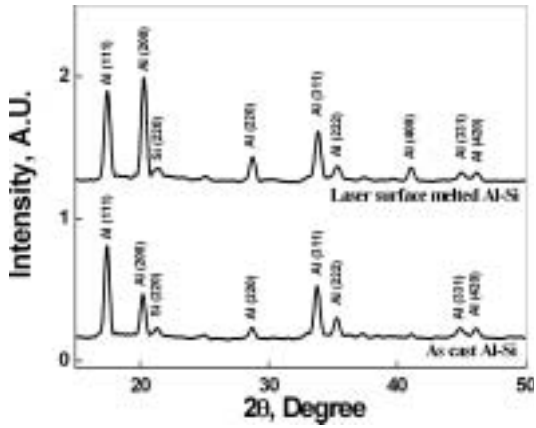

FIGURE 7
X-ray diffraction profiles of the top surface of as-cast and laser surface melted Al-11 wt.% Si alloy lased with a power of 2.3 kW and scan speed of 12 mm/min.

Figure 7 shows the x-ray diffraction profiles of as-received and laser surface melted Al-11 wt.% Si alloy t a power of 2.3 kW and a scan speed of 6 mm/min. On obtaining the x-ray at a diffraction profiles, it is necessary that oxidation was fully avoided under lasing conditions. A close comparison of the X-ray diffraction profiles between as-received and the laser surface melted Al-11 wt.% Si shows that there is marginal broadening of the Al peak after laser surface melting, which is attributed to grain refinement and the introduction of micro-strain due to the difference in thermal properties between Si and Al. The calculated lattice strain using Scherrer's formula was approximately 0.427% and did not vary significantly with scan speed.

Properties of the Melted Zone

A detailed evaluation of the microhardness at the surface and along the cross section of laser surface melted Al-11 wt.% Si alloy as a function of scan speed was undertaken. Figure 8 shows the variation in microhardness of the melted zone with the depth from the surface of laser surface melted Al-11 wt.% Si alloy at a power of 2.3 kW and a scan speed of 6 mm/min (plot 1), 9 mm/min (plot 2) and 12 mm/min (plot 3), respectively. In Figure 8 it is evident that the microhardness of the melted zone is significantly larger, 85 VHN as compared to 55 VHN of the as-received substrate. Furthermore, the microhardness varied marginally with a change in scan speed, which is possibly due to a change in grain size and volume fraction of the eutectic. However, a detailed correlation in this regard has not been made. Almost uniform microhardness with depth demonstrates the presence of almost uniform grains with depth. Hence, it may be concluded that laser surface melting could lead to the formation of a hard surface with almost uniform hardness throughout. The mechanism of

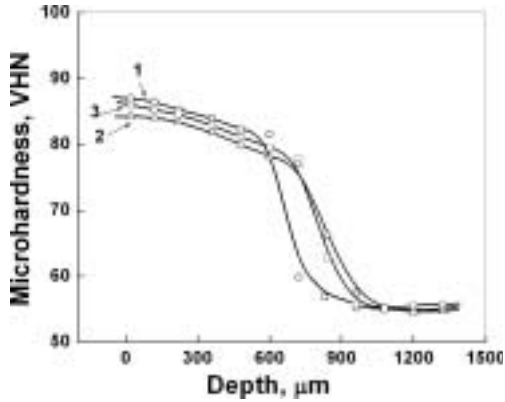

FIGURE 8
Variation of microhardness with depth from the surface of laser surface melted Al-11 wt.% Si alloy lased with a power of 2.3 kW and scan speed of (a) 6 mm/s, (b) 9 mm/s and (c) 12 mm/s, respectively.

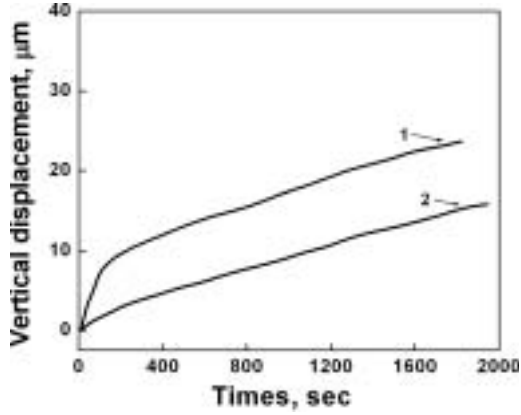

FIGURE 9
Variation of wear loss (in terms of depth of wear) as a function of time for as received and laser surface melted Al-11 wt.% Si alloy lased with a power of 2.3 kW and scan speed of 6 mm/s.

hardening was mainly grain refinement and presence of fine silicon distributed throughout the microstructure.

Figure 9 shows the variation of wear loss (in terms of depth of wear or vertical displacement) as a function of time for as received and laser surface melted Al-11 wt.% Si alloy lased with a power of 2.3 kW and scan speed of 6 mm/s. Figure 9 shows that the rate of wear is significantly reduced due to laser surface melting. The improved wear resistance of the laser surface melted Al-Si alloy is attributed to grain refinement and hence, increased hardness.

Table 1 summarises the calculated values of corrosion rate derived from the potentiodynamic polarisation studies of the as-received and laser surface

Sample history	Environment	Corr rate mm/yr
As received Al-11 wt.% Si	1M H_2SO_4	$2.154*10^{-1}$
Laser surface melted Al-11 wt.% Si		$8.149*10^{-1}$
As received Al-11 wt.% Si	1M HNO_3	$1.33*10^{1}$
Laser surface melted Al-11 wt.% Si		$2.55*10^{0}$
As received Al-11 wt.% Si	3.5% NaCl	$5.738*10^{-2}$
Laser surface melted Al-11 wt.% Si		$1.57*10^{-1}$

TABLE 1
Summary of Corrosion Behaviour of As-received vis-à-vis Laser Surface Melted Al-11 wt.% Si Alloy

melted Al-11 wt.% Si alloy in a different environment. A detailed analysis of the corrosion data in Table 1 reveals that laser surface melting shows different corrosion behaviour in different environments. In a 3.5 wt.% NaCl solution the corrosion resistance property is very poor with almost one order of magnitude increase in the corrosion rate. On the other hand, in H_2SO_4 environment too there is increase in corrosion rate to almost two times as compared to the as-received Al-11 wt.% Si alloy. However, a significant improvement in corrosion resistance (in terms of an order of magnitude reduction in corrosion rate) when laser surface melted material is put into a HNO_3 containing environment. In this regard, it is relevant to mention that Wong and Liang [11] reported the enhancement of corrosion resistance both in 10% H_2SO_4 and 10% HNO_3 solution due to the presence of silicon in solid solution. Furthermore, they also reported that in presence of chloride ions significantly damaged the Al_2O_3 film and caused the formation of $NaAlO_2$ [11]. However, in the present study a detailed investigation of the different corrosion behaviours between a laser surface melted specimen and the as-received alloy has not been undertaken.

SUMMARY AND CONCLUSIONS

From the present study the following conclusions may be drawn:

1 Laser surface melting of Al-11 wt.% Si alloy has been carried out with a 2.3 kW power and scan speed ranging from 6–12 mm/s.

2 Laser surface melting leads to the formation of a refined microstructure with dendritic or cellular morphology.

3 The microstructure of the melted zone consists of grain refined Al and Al-Si eutectic colonies.

4 The microhardness of the melted zone was significantly improved to 85 VHN as compared to that of 55 VHN of the as-received Al-Si alloy.

5 The wear resistance of the melt surface was improved significantly as compared to as-received Al-Si alloy.

6 A detailed corrosion study in 1M H_2SO_4, 1M HNO_3 and 3.56 wt.% NaCl solution shows that corrosion resistance was significantly improved in 1M HNO_3 solution. However, in 1M H_2SO_4 and 3.56 wt.% NaCl solution, corrosion property is deteriorated.

ACKNOWLEDGEMENT

Financial support for the project from Council of Scientific and Industrial Research (CSIR), N. Delhi, Department of Science and Technology (DST), N. Delhi and Board of Research on Nuclear Science (BRNS), Bombay are gratefully acknowledged.

REFERENCES

[1] Shabestari, S. G., Moemeni, H. (2004). *J. Mater. Process. Technol.* **30**, 193.

[2] Clapham, L. and Smith, R. W. (1987). *Acta metall.* **37**, 303.

[3] Draper, C. W. and Poate, J. M. (1985). *Int. Met. Rev.* **30**, 85.

[4] Molian, P. A. (Eds.) (1989). Surface Modification Technologies-An Engineer's Guide, New York, Marcel Dekker Inc., 1.

[5] Mordike, B. L. Mordike, Cahn, R. W., Haasan, P. and Kramer, E. J. (Eds.) (1993). Materials Science and Technology, Weinheim, VCH, 111.

[6] Dutta Majumdar, J. and Manna, I. (2003). Sadhana, **28**, 495–562.

[7] Rehn, L. E., Picraux, S. T. and Wiedersich, H. (Eds.) (1987). Surface Alloying by Ion, Electron and Laser Beams, Ohio, ASM, Metals Park, 1.

[8] Dutta Majumdar, J., Galun, R., Mordike, B. L. and Manna, I. (2003). *Mater. Sci. Engg.* **361**, 119–129.

[9] Noordhuis, J. and Hosson, J. Th. M. De. (1992). *Acta metall, mater.* **40**, 3317–3324.

[10] Wong, T. T., Liang, G. Y. and Tang, C. Y. (1997). *Journal of Materials Processing Technology*, **66**, 172–178.

[11] Wong, T. T. and Liang, G. Y. (1997). *Journal of Materials Processing Technology*, **63**, 930–934.

[12] Allen, D. R., Gremaud, M. and Perepezko, J. H. (1997). *Materials Science & Engineering A*, **A226–22**, 173–177.

[13] Watkins, K. G., McMahon, M. A. and Steen, W. M. (1997). *Maters. Sci. Engg.* **A231**, 55–61.

[14] Tomida, S., Nakata, K., Shibata, S., Zenkouji, I. and Saji, S. (2003). *Surface and Coating Technology*, **169–170**, 468–471.

[15] Fontana, M. G. (Eds.) (1987) Corrosion Engineering, New York, McGraw-Hill, 71.

[16] Reed Hill, R. E. and Abbaschian, R. (Eds.) (1992) Physical Metallurgy Principles, Boston, PWS-Kent Pub.